

The Hartree–Fock–Heitler–London Method, III: Correlated Diatomic Hydrides

Giorgina Corongiu*

Dipartimento di Scienze Chimiche ed Ambientali, Università dell’Insubria, Via Lucini 3, I-22100, Como, Italy
Received: February 13, 2007; In Final Form: April 9, 2007

In a recently proposed model, called Hartree–Fock–Heitler–London (HF–HL) (Corongiu, G. *J. Phys. Chem. A* 2006, 110, 11584), the molecular wave function was variationally obtained by merging two traditional models, Hartree–Fock (HF) and Heitler–London (HL). In the new method, the non-dynamical correlation energy—which includes state avoided crossing—is explicitly calculated with a few configurations. In this work the dynamical correlation energy for diatomic hydrides of the first and second period is computed both *ab initio*, via short MC–HF and MC–HL expansions—including ionic and excited covalent structures—and semiempirically, using the Coulomb hole algorithm, a density functional proposed by Clementi in the early 1960s. The Coulomb Hole correction is applied to HF and HF–HL functions, and, departing from tradition, also to HL functions. Few *ab initio* HF–HL configurations with inclusion of ionic structures yield reasonable binding energies not only for the hydrides considered but also for the van der Waals HeH molecule. The computed binding energies (in kcal/mol) from HF–HL functions corrected with the Coulomb hole functional are as follows: 109.48 (109.48) for H₂[¹Σ_g⁺]; 0.01 (0.01) for HeH [²Σ⁺]; 59.22 (58.00) for LiH [¹Σ⁺], 49.55 (49.83) for BeH [²Σ⁺], 86.77 (84.1) for BH [¹Σ⁺], 82.65 (83.9) for CH [²Π], 81.57 (80.5) for NH [³Σ[−]], 107.18 (106.6) for OH [²Π], and 140.91 (141.5) for HF [¹Σ⁺]; experimental values are given in parentheses. The computed total energies are in good agreement with exact nonrelativistic values. The combined availability of the correlation and binding energies from HF, HL, and HF–HL models allows a novel analyses on the hydrides chemical bond, in agreement with accepted physical chemistry concept derived from MO and VB theories.

1. Introduction

The Hartree–Fock–Heitler–London (HF–HL) method with the discussion on its algorithms is presented in the first two papers of this series.^{1,2} The method variationally merges the Hartree–Fock^{3–7} (HF) and the Heitler–London⁸ (HL) methods. It also accounts for the nondynamical correlation energy, and avoided curve crossing, to yield the correct dissociation products (see detailed discussions in ref 2). Thus, the HF and HL are proto-models for the HF–HL model.

In this work, we mainly consider the computation of the dynamical correlation energy, using either *ab initio* short multiconfiguration (MC) expansions or density functional formalism, applied to first and second period diatomic hydrides. A study of homopolar diatomic molecules of the first and second period will be the subject of a forthcoming paper.⁹ We are also looking at applying this method to polyatomic molecules.

The HF–HL method has been presented^{1,2} as a three-step approach; the first step merges HF and HL functions, replacing them with MC–HF and MC–HL short expansions to treat 2s–2p near-degeneracy^{10–13} and/or curve crossing; the second step extends the above MC expansions to fully correlate valence electrons and improves the compute binding energy by including ionic structures; the third step extends these expansions to also correlate inner shell electrons. An additional extended MC–HF atomic expansion can be added to the HL component to improve the computed correlation energy (see ref 1 for preliminary results). As alternative to the *ab initio* approach, the goals of the second and third step can be met semiempirically, using density functionals. We will refer to the second and third steps as “post HF–HL” computations—in analogy to “post-HF” computations.

This paper is organized as follows: the *ab initio* addition of ionic structures is discussed in Section 2; the computation of van der Waals bonds in Section 3; the inclusion of the Coulomb hole density functional in Section 4; comments on the correlation energy correction in Section 5; finally, the laboratory binding energy pattern is compared to the computations in Section 6, providing a physical and chemical explanation of the X–H chemical bond.

2. Extension of the HF–HL First Step *ab initio* Formalism

The correlation energy, E_c , is often partitioned² into nondynamical, $E_c(\text{non-dyn})$ and dynamical, $E_c(\text{dyn})$:

$$E_c = E_c(\text{non-dyn}) + E_c(\text{dyn}) \quad (1)$$

As $E_c(\text{non-dyn})$ is included in the first HF–HL step,² we will focus on computation of $E_c(\text{dyn})$. In *ab initio* computations, the goal is usually to compute the total correlation energy, E_c , but if this is too complex or unnecessary, it is possible to limit this to the binding energy part of the correlation correction, the so-called “molecular extra correlation energy”,¹⁴ denoted as η_M . Recall that the correlation energy can be decomposed into the molecular extra correlation energy and the sum of the atomic correlation energies, ϵ_a :

$$E_c = \eta_M + \sum_a \epsilon_a \quad (2a)$$

The two terms in the left side of eq 2a can be partitioned into the dynamical and nondynamical components

$$E_c = \eta_M(\text{dyn}) + \eta_M(\text{non-dyn}) + \sum_a [\epsilon_a(\text{dyn}) + \epsilon_a(\text{non-dyn})] \quad (2b)$$

TABLE 1: Hydrides: Laboratory Binding Energies (kcal/mol), Equilibrium Internuclear Separations (bohr) and Total Nonrelativistic Energies (hartree) Compared with Computed Binding Energies (kcal/mol) from HF, HL, and First-Step HF-HL

molecule	E_b^a	R_c^a	$E_T[R_c]$	$E_b(\text{HF})$	$E_b(\text{HL})$	$E_b(\text{HF-HL})$
H ₂ [$^1\Sigma_g^+$]	109.48 ^b	1.4 ^b	-1.1744757	83.83	94.28	94.50
HeH [$^2\Sigma^+$]	0.01 ^c	7.00 ^c	-3.4037459	-0.0	-0.0	-0.0
LiH [$^1\Sigma^+$]	58.00	3.0150	-8.070491	34.27	43.11	43.66
BeH [$^2\Sigma^+$]	49.83 ^d	2.5371	-15.246792	40.2, ^e 50.29	-29.25	40.50
BH [$^1\Sigma^+$]	84.1 ^f	2.3289	-25.28792	64.35	72.18	77.78
CH [$^2\Pi$]	83.9	2.1163	-38.47868	57.14	65.82	70.03
NH [$^3\Sigma^-$]	80.5 ^g	1.9582	-55.21756	48.59	57.30	60.29
OH [$^2\Pi$]	106.6	1.8324	-75.73726	70.16	72.26	79.62
FH [$^1\Sigma^+$]	141.5 ^h	1.7325	-100.45962	101.23	92.17	108.36

^a Reference 20. ^b Reference 21. ^c References 22 and 23. ^d Reference 24. ^e Reference 2. ^f Reference 25. ^g Reference 26. ^h Reference 27.

For the HF-HL model² this reduces to

$$E_c(\text{dyn}) = \eta_M(\text{dyn}) + \sum_a \epsilon_a(\text{dyn}) \quad (3)$$

From eqs 2 and 3, it follows that the exact binding energy, E_b , is the sum of $\eta_M(\text{dyn})$ and the computed binding energy from a given model (like HF or HL), $E_b(\text{model})$:

$$E_b = \eta_M(\text{dyn}) + E_b(\text{model}) \quad (4)$$

We shall use eq 4 in the discussion of the computed binding energies in Section 6. From the above considerations, it appears that it would be of interest the computation of $\eta_M(\text{dyn})$ independently from $\sum_a \epsilon_a(\text{dyn})$. This consideration becomes very relevant when the difference between $\sum_a \epsilon_a(\text{dyn})$ and $\eta_M(\text{dyn})$ is very large, as it is the case for van der Waals binding.

It is known^{2,15} that the addition of ionic structures to the covalent configuration in the HL component of the HF-HL function improves the prediction for the binding energy, reducing $\eta_M(\text{dyn})$ and increasing $E_b(\text{model})$. For the LiH molecule, as an example, ionic structures are Li^+H^- and Li^-H^+ with corresponding configurations $1s^2_{\text{Li}}[1\text{S}]1s^2_{\text{H}}[1\text{S}]$ and $1s^2_{\text{Li}}2s^2_{\text{Li}}[1\text{S}]1s^0_{\text{H}}$.

Ionic structures were not included in the first HF-HL step—as part of the HL component—as this would have accounted for some of the total dynamical correlation, a task left to post HF-HL computations. For HF-HL functions, we use the term “structure” as an alternative to the term “configuration of the HL component” and we retain the designation “configuration” for the HF component. Incidentally, ionic structures were first used in quantum chemical computations in a paper by Majorana¹⁶ in 1931. Majorana attempted to improve the celebrated Heitler-London computation⁸ by adding the H^+H^- structure with a $2p_\sigma$ orbital in the H^- configuration.

For the HX hydrides, the ionic structures H^-X^+ and H^+X^- are designated “basic ionic” structure when they dissociate either into H^- in the ^1S ($1s^2$) state and X^+ , or H^+ and X^- . The ions X^+ and X^- are in the lowest ionic configuration state, and fulfill the Wigner-Witmer¹⁷ and Mulliken¹⁸ dissociation rules analyzed in the classical volume by G. Herzberg.¹⁹ When the ions are not in the lowest ionic configuration, we use the designation “Majorana structure”. We call the structures not dissociating into the lowest configuration “excited covalent” structures. In this work we will make use of covalent, covalent excited, basic ionic and Majorana structures (see also Table 2 of ref 2).

Table 1 reports the following data (discussed in ref 2) for the hydrides analyzed in this work: laboratory binding energies, E_b ; internuclear equilibrium distances, R_c ; exact nonrelativistic energies at equilibrium, $E_T(R_c)$; binding energies previously obtained from HF, $E_b(\text{HF})$, HL, $E_b(\text{HL})$, and first step HF-HL computations, $E_b(\text{HF-HL})$. The large basis sets utilized reproduce the HF atomic limit; the added polarization functions not

TABLE 2: Computed Binding Energy (kcal/mol), $E_b(\text{HF-HL})_i$, Total Energies (hartree) at Equilibrium, $E(\text{HF-HL})_i(R_c)$, and at Dissociation, $E(\text{HF-HL})_i(R_\infty)$, from HF-HL with Ionic Structures

molecule	$E_b(\text{HF-HL})_i$	$E(\text{HF-HL})_i(R_c)$	$E(\text{HF-HL})_i(R_\infty)$
H ₂ [$^1\Sigma_g^+$]	95.42	-1.15207	-1.00000
HeH [$^2\Sigma^+$]	0.17	-3.37826	-3.37799
LiH [$^1\Sigma^+$]	46.59	-8.00699	-7.93274
BeH [$^2\Sigma^+$]	45.73	-15.18961	-15.11673
BH [$^1\Sigma^+$]	78.10	-25.18831	-25.06384
CH [$^2\Pi$]	78.39	-38.33102	-38.20610
NH [$^3\Sigma^-$]	71.50	-55.01548	-54.90153
OH [$^2\Pi$]	98.11	-75.46883	-75.31028
HF [$^1\Sigma^+$]	136.12	-100.12830	-99.91136

only yield the HF molecular limit, but also reasonably correlated CASSCF functions.² We recall that the “exact” nonrelativistic energies are obtained by adding the experimental binding energy, corrected for relativistic effects, to the “exact” nonrelativistic energies²⁸ of the separated atoms. Likely, the number of figures given in the Table reflects more numerical than physical accuracy.

Using the basis sets given in ref 2, we have added the “basic ionic” structures to the first step HF-HL functions. The gain in the binding energy relatively to HF-HL covalent computations is appreciable, as shown in Figures 1 and 2a,b and also in Table 2. In the table we report the computed binding energy, indicated as $E_b(\text{HF-HL})_i$, computed total energy at equilibrium, $E(\text{HF-HL})_i(R_c)$, and at dissociation, $E(\text{HF-HL})_i(R_\infty)$.

In Figure 1 we compare the computed binding energy from the HF, and first step HF-HL (without and with “basic ionic” structures), to the laboratory binding energies. In Figure 2a we report the computed potential energy curves for H₂, LiH, BeH, BH; in Figure 2b we continue with the hydrides CH, NH, OH, and HF. In Figure 2a,b the notation HF-HL is equivalent to the redundant notation (HF-HL)(1,1); the specification “-ionic”

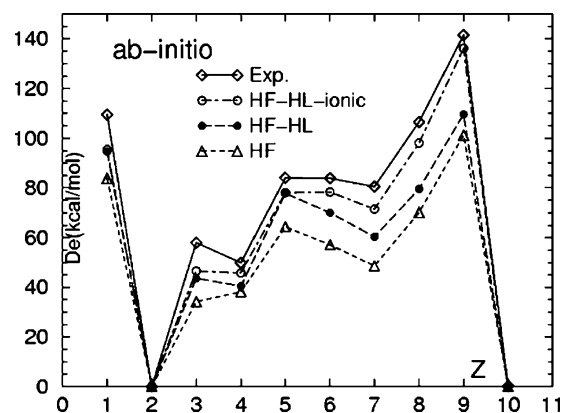


Figure 1. Hydride binding energies from HF, HL, first step HF-HL, without and with “basic ionic” structures, compared to laboratory data.

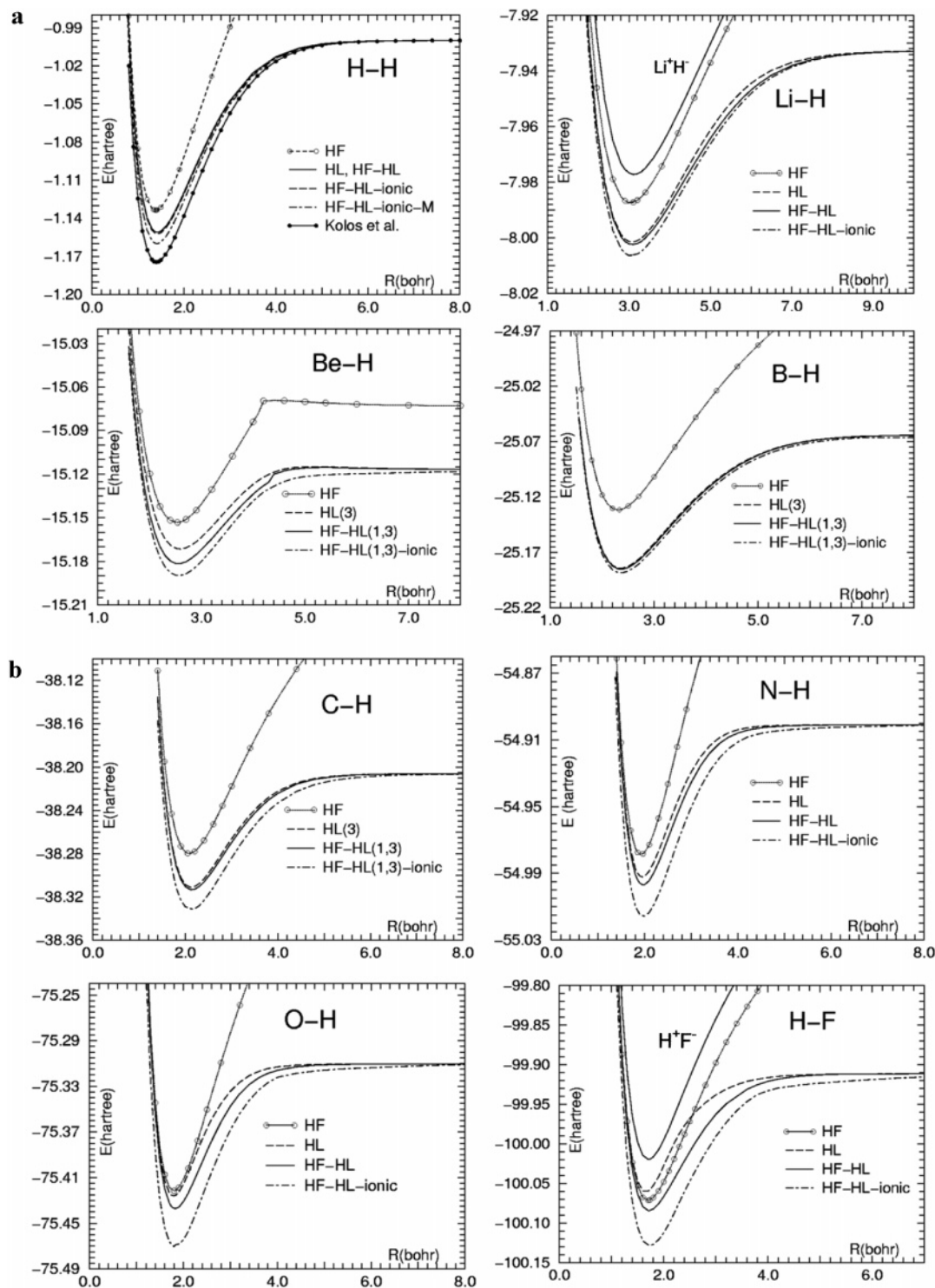


Figure 2. a. Potential energy curves for H₂, LiH, BeH, and BH, from HF, HL, first step HF-HL without and with “basic ionic” structures. b. Potential energy curves for CH, NH, OH, and HF, from HF, HL, first-step HF-HL without and with “basic ionic” structures.

indicates addition of basic ionic structures to the (HF-HL)(m,n) function (see ref 2 for the notation).

In the H₂ inset of Figure 2a the notation HF-HL-ionic-M refers to computations with the addition to the covalent HF-HL function of the Majorna structure $H^-(2p_{\sigma}^2; ^1S) H^+$; the corresponding binding energy is 100.24 kcal/mol compared to 95.42 from the computation with the basic ionic structure, and 94.50 for the covalent HF-HL function; the latter is indistinguishable in the figure from the HL binding, which is 94.28 kcal/mol. We have added the results of Kolos et al.²¹ for comparison. For LiH we have added the potential energy curve

obtained with the basic ionic structure $Li^+(^1S; 1s^2)H^-(^1S; 1s^2)$ optimized alone—without the presence of the covalent structure. This is indicated in the inset with the label Li^+H^- . For BeH, the state crossing and near-degeneracy require three covalent structures to be considered in the HL component (see ref 2 for details). The addition of the ionic structures creates significant energy changes, yielding a binding energy of 46.59 kcal/mol.

For all “HF-HL-ionic” curves presented in Figure 2b, the ionic structure contribution is important. For the HF hydride, we also report the potential energy curve for the ionic structure H^+F^- computed independently from the covalent one (indicated in

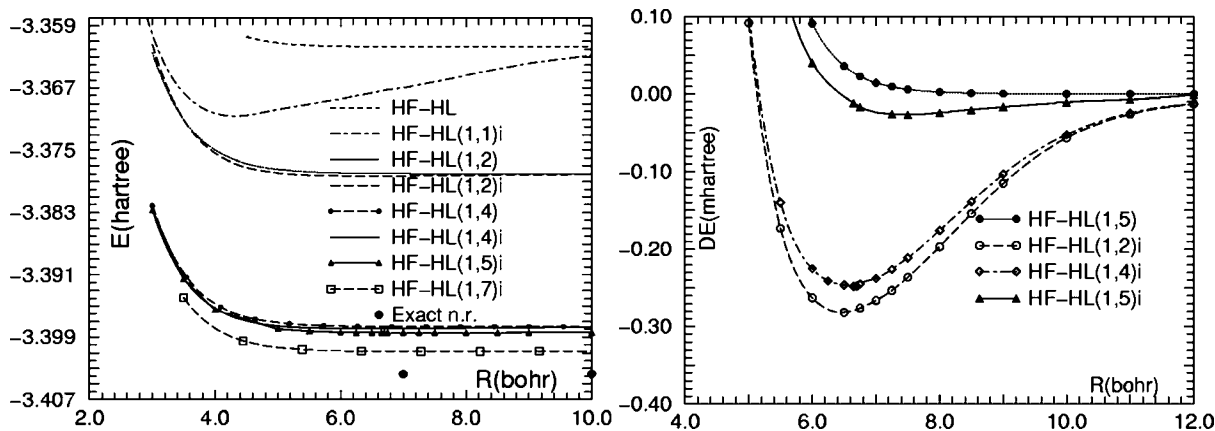


Figure 3. Potential energy curves for HeH. Left: HF-HL and HF-HL-ionic (energies in hartree). Right: details for the binding region (energies in mhartree). See text.

the inset with the label H^+F^-). Analysis of these computations is given in Section 6.

The inclusion of ionic structures reported in this work can be considered as a preliminary step for a more general analyses of in-out correlation. We believe this can be related to the atomic radial correlation energy calculated for the first and second row atoms by Clementi et al.²⁹ using non orthogonal orbitals.

The ground-state atomic configurations are standard references in HF and HL computations. With the inclusion of near-degeneracy we have consider excited neutral atom configurations, for example, $1s^22s^02p^{2+n}$ in addition to $1s^22s^22s^n$, and with state crossing we consider additional excited configurations. Finally, the inclusion of ionic structure means we must consider positive and negative ionic configurations. In essence, we are introducing relatively few but carefully selected configurations, present in full CI or CASSCF systematic expansions, which are, however, very extended, and likely redundant being “machine” generated.

3. Van der Waals Molecules

In ref 2 we reported HeH computations with the CASSCF technique; the computed molecular binding is 0.0211 mhartree, in substantial agreement with laboratory²² and computed²³ data, ranging from 0.0215 to 0.0227 mhartree; in the CASSCF computations, the selected full active space leads to over one million determinants.

HeH is considered below with the HF-HL second step ab initio methodology. The van der Waals molecule HeH provides a nice example of a binding where $\sum_a \epsilon_a(\text{dyn}) \gg \eta_M(\text{dyn})$, specifically 0.04207 hartree versus 0.022 mhartree. Thus, in the HF-HL second step we expect that the variational technique adopted in optimizing the orbitals in variational expansions, will tend to satisfy first $\epsilon_a(\text{dyn})$ and second $\eta_M(\text{dyn})$.

The HL component of the HF-HL function is constructed with the standard covalent HF-HL first step configuration $He-(^1S;1s^2)H(^2S;1s^1)$, yielding the (HF-HL)(1,1) function, denoted C1 for short. We have considered the following additional configurations: the ionic structures $He^{-(^2S;1s^22s^1)H^+}$ and $He^{+(^2S;1s^1)H^{-(^1S;1s^2)}}$ denoted Ci, the excited covalent configuration $He(^2S;1s^12s^1)H(^2S,1s^1)$ denoted C2, the two excited covalent function $He(^2S;1s^02p_\sigma^2)H(^2S,1s^1)$ and $He(^2S;1s^02p_\pi^2)H(^2S,1s^1)$, denoted C3 and C4, respectively, and a covalent excited configuration $He(^2S;1s^13s^1)H(^2S,1s^1)$ denoted C5. The configurations from C2 to C5 are expected to account mainly for $\epsilon_a(\text{dyn})$, whereas Ci is expected to account for $\eta_M(\text{dyn})$. Our orbital optimization technique, being carried out without orthogonality constraint, imposes a gradual build up in

the configuration expansion. For example the optimization of a 3s orbital for C5 requires the presence of a 2s orbital (present in the C2 configuration) since its absence could bring about a 2s rather than a 3s orbital. As we shall see, both the 2s and 3s are important for $\epsilon_a(\text{dyn})$. Thus to obtain $\eta_M(\text{dyn})$ we are forced to obtain also $\epsilon_a(\text{dyn})$.

In Figure 3 we report on the gradual build up of the HF-HL function to obtain $\eta_M(\text{dyn})$ for HeH. We present the computed potential total energy curves (left inset) and some of the corresponding binding energy curves (right inset), the latter reported relatively to their own dissociation energy, thus all with the same zero. The (HF-HL)(1,1) function yields the previously reported² repulsive potential energy curve (see left inset of Figure 3). The total energies are -3.361659 hartree at 6.65 bohr and -3.361679 at dissociation.

The combination of C1 and Ci yields the (HF-HL)(1,1)i function with an attractive potential energy curve (see Figure 3) with a minimum at 4.32 bohr and a binding of 0.00889 hartree. The ionic structures He^+H^- and He^-H^+ bring about electrostatic attraction; in addition, the $He^{+(^2S;1s^1)H^{-(^1S;1s^2)}}$ structure brings about the negative ion H^- stabilization energy relative to neutral atom $H(^2S;1s^1)$. Concerning the short internuclear distance of the computed minimum for (HF-HL)(1,1)i, we note that $He^{-(^2S;1s^22s^1)H^+}$ corresponds to the united atom for the HeH ground state, the Li electronic structure $[^2S](1s^2-2s^1)$. The ionic structure overshoots the binding, yields a minimum at far too short distance and does not affect $\epsilon_a(\text{dyn})$ at dissociation.

The combination of C1 and C2 yields the (HF-HL)(1,2) function. This function has a considerable energy stabilization relative to (HF-HL)(1,1), but yields a repulsive potential curve with no minimum. The He atom is partly correlated: the correlation energy error in (HF-HL)(1,2) it is reduced to -0.02573 hartree at dissociation with a repulsive interaction of 0.03 mhartree at 6.65 bohr. The overall result is a shift to lower energies relative to the potential energy curve of (HF-HL)(1,1), namely, a correlation gain in $\epsilon_a(\text{dyn})$, and not in $\eta_M(\text{dyn})$, as shown in the left inset of Figure 3.

The addition of Ci to (HF-HL)(1,2) yields (HF-HL)(1,2)i with a potential energy curve very near to the one for (HF-HL)(1,2); the new computation has a minimum at about 6.43 bohr with a depth of 0.28 mhartree. This value is 1 order of magnitude larger than the CASSCF result² or the experimental values,^{22,23} and its minimum occurs at a somewhat more reasonable distance relatively to the one from (HF-HL)(1,1)i. It appears that this function improves $\epsilon_a(\text{dyn})$ and marginally $\eta_M(\text{dyn})$, pointing to the existence of binding in this region, as shown in the right

inset of Figure 3; unfortunately the need to improve $\epsilon_a(\text{dyn})$ is variationally dominating, leading to an exaggerated apparent binding. The competition between $\eta_M(\text{dyn})$ and $\epsilon_a(\text{dyn})$ reminds us of the basis set superposition error problem, where a basis function, introduced to improve a given atom representation, is instead used by the variational technique to improve the representation on a different atom. Therefore, other excited configurations are needed to shift the apparent minimum toward larger distances and to balance the two correlation corrections, $\epsilon_a(\text{dyn})$ and $\eta_M(\text{dyn})$.

Addition to (HF-HL)(1,2) of the two excited covalent functions C3 and C4, yielding the function (HF-HL)(1,4), brings the total energy near to the exact nonrelativistic value, -3.39766 hartree at dissociation, but the minimum is no longer present (see Figure 3). Thus, $\epsilon_a(\text{dyn})$ is nearly accounted for, but not $\eta_M(\text{dyn})$. Addition to (HF-HL)(1,4) of the ionic structure Ci yields (HF-HL)(1,4)i; this function presents once more a minimum, still too deep, 0.25 mhartree, relative to experimental data (see Figure 3 right inset), even if less so relatively to the one from the (HF-HL)(1,2)i computation.

Finally, we have added to (HF-HL)(1,4)i the covalent configuration C5, yielding (HF-HL)(1,5)i. This computation at dissociation and at the internuclear separation of 7.00 bohr yields the total energies of -3.398441 and -3.398461 hartree, with a binding energy of 0.020 mhartree to be compared to the experimental value of 0.022 mhartree. The unaccounted correlation error, both at dissociation and equilibrium, is 5.28 mhartree. Thus, for the van der Waals binding energy—after having accounted for a large traction of $\epsilon_a(\text{dyn})$ —the HF-HL variational method finally starts to account also for $\eta_M(\text{dyn})$.

Additional configurations are needed to reach accurate nonrelativistic energies. Preliminarily, we have considered the addition of the following structures $\text{He}(1s^03d^2)\text{H}(1s^1)$, $\text{He}(1s^0-3p_\sigma^2)\text{H}(1s^1)$, $\text{He}(1s^03p_\pi^2)\text{H}(1s^1)$. The total energies at 7.50 bohr and at dissociation are -3.400789 and -3.400767 hartree, respectively, with a binding of 0.022 mhartree; the corresponding unaccounted correlation correction at dissociation is 2.96 mhartree. These computations, indicated in the left inset of Figure 3 with square marks, are not reported on the right inset since overlapping the HF-HL(1,5)i curve.

This set of computation on HeH shows that the HF-HL model can lead to the determination of the correct for van der Waals forces, using relatively few configurations. By reporting the computations in full detail we have exemplified the competing effects in accounting for $\epsilon_a(\text{dyn})$ and $\eta_M(\text{dyn})$. Preliminary computations of the van der Waals binding energy for NeH point to the equivalent trends.

4. Post-HF-HL Via a Density Functional

As stated in Section 2, in the HF-HL proposal the dynamical correlation can be introduced with a variety of alternative techniques either ab initio or semiempirically.³⁰ Extensive computations by Lie et al. for diatomic homopolar molecules³¹ and hydrides³² have shown that density functionals applied to MC expansions (computed to correct the HF function near dissociation), yield reasonable binding and total energies. The study by Wang and Schwarz³³ supports these findings with formal considerations. For HF-HL functions, the correct dissociation is ensured by construction; thus, a number of available and tested semiempirical density functionals^{34–46} can be used to account for the dynamical correlation. These functionals are all explicit corrections to HF wave functions; we call these techniques “DFA”, Density Functional Approximations, to distinguish them from Density Functional Theory (DFT), where

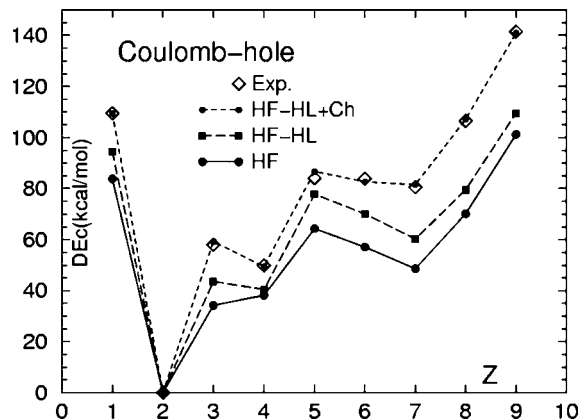


Figure 4. The binding energy obtained with the Coulomb hole, HF-HL+Ch, compared to experimental, HF, and HF-HL data from the first step.

TABLE 3: Coulomb Hole Computed Binding Energy (kcal/mol), $E_b(\text{HF-HL})\text{-Ch}$, the Total Energy (hartree) at Equilibrium, $E(\text{HF-HL})\text{-Ch}(R_e)$, and at Dissociation, $E(\text{HF-HL})\text{-Ch}(R_\infty)$, Deviation, ΔE , (kcal/mol) of the Latter from Exact Nonrelativistic Energies, Computed Equilibrium Separation in Bohr, $R_e\text{-Ch}$

molecule	$E_b(\text{HF-HL})\text{-Ch}$	$E(\text{HF-HL})\text{-Ch}(R_e)$	$E(\text{HF-HL})\text{-Ch}(R_\infty)$	ΔE	$R_e\text{-Ch}$
$\text{H}_2 [^1\Sigma_g^+]$	109.48	-1.17447	-1.00000	0.00	1.40
$\text{LiH} [^1\Sigma^+]$	59.22	-8.07236	-7.97798	0.05	3.01
$\text{BeH} [^2\Sigma^+]$	49.55	-15.24611	-15.16716	0.13	2.59
$\text{BH} [^1\Sigma^+]$	86.77	-25.29208	-25.15382	0.07	2.33
$\text{CH} [^2\Pi]$	82.65	-38.47601	-38.34429	0.44	2.11
$\text{NH} [^2\Sigma^-]$	81.57	-55.21857	-55.08846	0.50	1.93
$\text{OH} [^2\Pi]$	107.18	-75.73765	-75.56685	0.22	1.80
$\text{HF} [^1\Sigma^+]$	140.91	-100.45867	-100.23412	-0.26	1.68

the aim is to represent the atomic and molecular systems directly with the electronic density^{47,48} and not with wave functions.

In the Hartree–Fock (HF) model, the Coulomb interaction is overestimated, since the same orbital is used for two electrons. The Coulomb hole, Ch, is a density functional of DFA type,^{34,42,44} which attempts to correct the HF overestimate by replacing the $1/r_{12}$ operator with the operator $[1 - \exp(-\alpha r_{ij}^2)]/r_{ij}$ with α a semiempirical parameter. There are different algorithms for the Coulomb hole; in this work we use a molecular soft Coulomb hole, Ch, functional⁴⁴ previously tested after a calibration using atomic ionization potential, and molecular binding energies. Here, the parameter α is marginally re-calibrated, using available and reliable atomic correlation energy estimates,²⁸ the equilibrium energy of H_2 from Kołos et al.,²¹ and atomic energy data corrected for the 2s/2p near degeneracy, since we use the functional not on Hartree–Fock but on HF-HL wave functions. The re-calibration is presently in progress,⁴⁹ since we wish to test it on a larger sample of molecules, not restricted to hydrides.

The binding energy data obtained with the DFA Coulomb hole are displayed in Figure 4. The agreement with experimental data is good, particularly since the entire approach is obtained with few HF-HL configurations and a simple DFA correction. In Table 3 we report the computed equilibrium distance, R_e , the binding energy, $E_b(\text{HF-HL})\text{-Ch}$, the total energy at equilibrium, $E(\text{HF-HL})\text{-Ch}(R_e)$, and at dissociation, $E(\text{HF-HL})\text{-Ch}(R_\infty)$, the deviation, $\Delta E(\infty)$, between the latter values and exact nonrelativistic energies. These deviations show that the Ch parametrization is reliable for atoms.

In Figure 5a,b we report the HF-Ch, HL-Ch, and HF-HL-Ch potential energy curves for the hydrides. To ease comparison, in each inset we have added the exact nonrelativistic values at

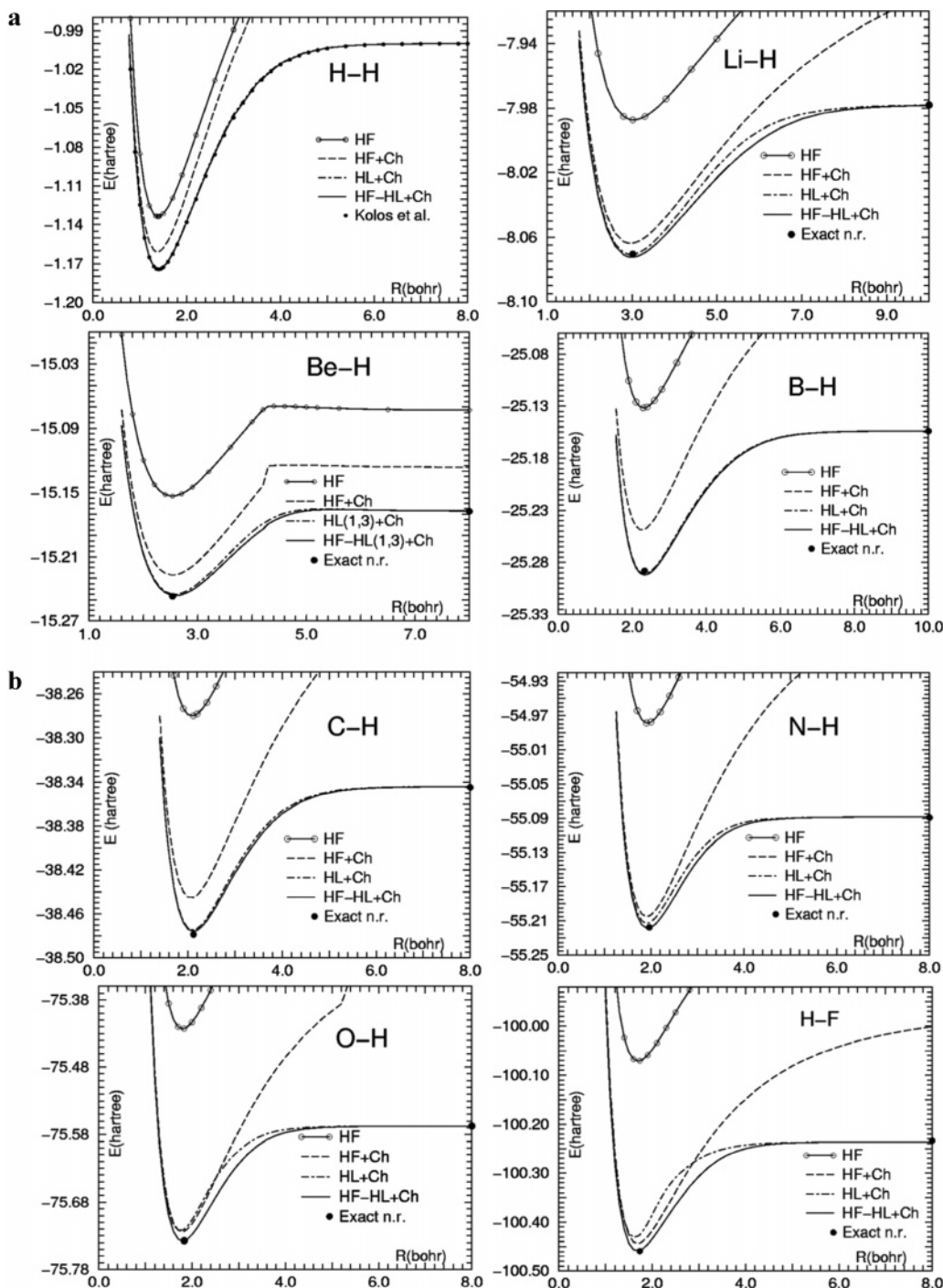


Figure 5. a. HF, HF-Ch, HL-Ch, and HF-HL-Ch potential energy curves for H_2 , LiH, BeH, and BH, and exact nonrelativistic energies at equilibrium and dissociation. b. HF, HF-Ch, HL-Ch, and HF-HL-Ch potential energy curves for CH, NH, OH, and HF, and exact nonrelativistic energies at equilibrium and dissociation.

equilibrium and dissociation. The results show good accuracy but also some residual small errors collected in Table 3. We recall that for an atom in the HF approximation the $2p$ electrons are degenerate, but in the molecule they split into $2p_\sigma$ and $2p_\pi$ due to the linear symmetry; this splitting, at dissociation, brings about a small correlation effect relatively to computation for separated atom. Indeed, the molecular potential, which is for a particular component of an atomic multiplet, will lead to contamination of the atomic orbitals with higher angular momentum.⁵⁰ Further, in the molecular computation, the d and f polarization functions contaminate the s and p functions, respectively. At very large distances, when the atoms do not interact, tentatively we have constrained the orbital coefficients

to atomic symmetry via elimination of undesired contributions from polarization functions. This, numerically reduces the contamination, for example in the HF molecule the effect is reduced from ~ 1.40 to ~ 0.25 kcal/mol.

The Kolos et al. computed energies are accurately matched from the HF-HL-Coulomb hole approach for the full range of internuclear separations, including the highly repulsive region. However, note that the exact H_2 value at equilibrium has been used to fit the Ch functional. For BeH, the HF-Ch curve shows the characteristic discontinuity before dissociation, discussed at length in ref 2; the inclusion of the two crossing states eliminates the discontinuity at the crossing, as shown in ref 2 and in the HF-HL (1,3)-Ch potential energy curve.

TABLE 4: Correlation Energy for Hydrides at Equilibrium from HF, HF-HL, and (HF-HL)_i^a

molecule XH	$-E_c(\text{HF})$	$-E_c(\text{HF-HL})$	$-E_c(\text{HF-HL})_i$	$-E_c(\text{X})$	$-E_c(\text{X}^-)$	$-E_c(\text{X}^+)$
H ₂ [¹ Σ _g ⁺]	0.04087	0.02387	0.02372	0.00000	0.03951	0.00000
HeH [² Σ _g ⁺]	0.04209	0.04207	0.03318	0.04204	0.04204	0.00000
LiH [¹ Σ _g ⁺]	0.08315	0.06819	0.06349	0.04533	0.04532	0.04350
BeH [² Σ _g ⁺]	0.09363	0.06552	0.06352	0.05054	0.07785	0.04737
BH [¹ Σ _g ⁺]	0.15633	0.10012	0.09962	0.09014	0.13488	0.05252
CH [² Π]	0.19903	0.16098	0.14768	0.13869	0.18274	0.09592
NH [³ Σ _g ⁻]	0.23922	0.22055	0.29265	0.18834	0.26166	0.14483
OH [² Π]	0.31607	0.30011	0.27061	0.25798	0.33135	0.19427
FH [¹ Σ _g ⁺]	0.38895	0.37557	0.33137	0.32478	0.39954	0.26128

^a Correlation energies (hartree) for neutral atoms, positive, and negative ions corrected for near-degeneracy.

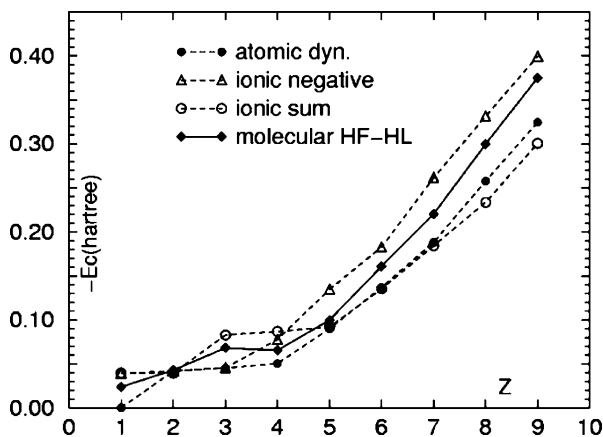


Figure 6. Correlation energy for molecular HF-HL (solid line), neutral atom dissociation products (atomic dyn.), ionic structure dissociation products $[\text{H}^-] + [\text{X}^+]$ (ionic sum), and $[\text{H}^+] + [\text{X}^-]$ (ionic negative).

The HF-HL-Ch results are superior to those for HF-Ch or HL-Ch, due to the higher accuracy obtained in the HF-HL function and to the calibration of Ch functional, aimed at HF-HL functions. From Figure 5a,b we can see that the HF-Ch and the HL-Ch binding conserve the trend found for HF and HL energies, and tend to slightly shift the equilibrium position. Thus, for example in hydrogen fluoride, the HL equilibrium position shift to shorter internuclear separations is partially retained in the HF-HL-Ch potential.

We wish to recall that in literature there are many density functionals, which can represent valid alternatives to those mentioned.^{34–46} A few^{51–60} are implemented in our code,^{49,61} but do require re-optimization of the parameters being the calibration rather old and not designed for HF-HL functions.

5. HF-HL Correlation Energies

From eq 4 we know that the molecular binding is the sum of a contribution from the binding obtained with a given ab initio model, $E_b(\text{model})$, and the correlation correction, η_M , associated to the model. Whereas, traditionally the $E_b(\text{model})$ is stressed, below we consider η_M in the HF, HL, HF-HL approximations, thus we stress the correlation energy correction, not only in the molecule, but also in the atoms at dissociation, including the positive and negative ions participating to the ionic structures.

In Table 4, we report the correlation energies for HF, HF-HL, and (HF-HL)_i at equilibrium, and the ground state atomic and ionic correlations energies²⁸ corrected for near-degeneracy with our Gaussian basis set.²

Figure 6 (derived from the data in Table 4) shows a comparison of the dynamical correlation energy from the HF-HL computations at equilibrium (labeled “molecular HF-HL”), and the sum of the dynamical correlation energies of both the neutral atoms (labeled “atomic dyn.”) and the positive and

negative ions in their ground state (labeled “ionic sum” for H^-X^+ and “negative ion” for H^+X^-). For XH molecular computations, the correlation energy at dissociation is simply the atomic correlation energy of the atom X (the correlation of the H atom is zero). For ionic structures, we must consider the sum of the dynamical correlation energies for the positive and negative ions; for $[\text{H}^+] + [\text{X}^-]$ it is simply the value of the negative ion X^- but for $[\text{H}^-] + [\text{X}^+]$ it is the sum of the correlation energies²⁸ of $[\text{H}^-]$ (-0.03951 hartree) and of $[\text{X}^+]$. Since the HF-HL accounts for the 2s-2p non-dynamical correlation, from the atomic and ionic correlation energies we have subtract the near-degeneracy energy component.

The four sets of data reported in Figure 6 show that correlation energies increase with the number of electrons—as generally expected—but follow specific patterns. Some of the correlation energy values are very close and not easily distinguishable in the graph. For example, as expected, for the He atom the negative ion and the ionic sum for $\text{He}^+(^2\text{S}, 1\text{s}^1) + \text{H}^-(^1\text{S}; 1\text{s}^2)$ have essentially equal correlation energy. This is also the case - due to near degeneracy - for $\text{Li}^-(^1\text{S}, 1\text{s}^2 2\text{s}^1)$ compared to $\text{Li}^-(^1\text{S}, 1\text{s}^2 2\text{s}^2)$, for $\text{Be}^-(^2\text{P}) + \text{H}^+$ compared to $\text{Be}^+(^2\text{S}) + \text{H}^-(^1\text{S})$, and also for the boron, carbon and nitrogen neutral atoms compared to the $\text{X}^+ + \text{H}^-$ sum.

From BeH to HF, the molecular correlation at equilibrium is bracketed by the correlation values of the negative ions and the neutral atoms; for OH and HF, it is closer to the negative ion values. For LiH an inversion occurs, the value of the molecular correlation energy is bracketed between the neutral atom and the $\text{X}^+ + \text{H}^-$ ionic pair. For HeH the molecular HF-HL correlation is essentially equal to the neutral and to the ionic sums; the same holds for NeH. For H₂ the molecular correlation is smaller relative to both the ionic sum and the negative ion. From BH to HF, the sum of the ionic pair $\text{X}^+ + \text{H}^-$ correlation energies is close to the neutral atom value and starts to differ for oxygen and fluorine; this pattern is different for BeH and LiH (see Table 4). In the HF-HL model, the molecular correlation energy for H₂ is close to the value of H^- , for LiH and BeH to the values of X^+H^- , and from BH to HF to the value of X^- .

The analyses of Figure 6 leads us to conclude that for BH, CH, NH, OH, and HF there should be a $(\text{X}^- + \text{H}^+)$ ionic structure component. This is nearly absent in BeH and is replaced with the $(\text{X}^+ + \text{H}^-)$ ionic structure for LiH. For H₂ the molecular symmetry implies we must talk of “in-out” correlation and not of ionic structures. As mentioned before, E. Majorana¹⁶ first considered an ionic structure for the H₂ molecule and defined the $\text{X}^- - \text{H}^+$ as a “pseudopolar bond”.

These observations call to mind some old hypotheses, specifically the relevance of the electro-negativity concept (i.e., relations for the energy difference between neutral atoms, positive and negative ions) in the understanding of molecular binding;⁶² the novel aspect presented above is the relevance of

the correlation energy, a quantity unexplored in the Pauling and Mulliken time, and the importance of considering both the MO and the HL models.

6. Comments on the X–H Bond

Traditionally, in considering X–H molecules, with X from the H to Ne, we acknowledge for H–H a homopolar bond, for He–H and Ne–H van der Waals bonds, and for the molecules from LiH to HF heteropolar ionic bonds. However, here we consider the ten molecules without any recognizing the above subdivision, since this should result from the bond analyses based on our computed data, particularly the equilibrium separations and the computed binding.

In molecules, the binding energy results both from classical forces and quantum corrections with nearly equal weight.⁴¹ Recalling eq 4 we analyze the XH molecules using the values of $\eta_M(\text{dyn})$, one of the two components to the binding, and the computed binding of the HF, HL, HF-HL, and (HF-HL) models reported in Figures 1, 4, and 6 and in Table 4.

The equilibrium internuclear distances from the HF-HL computations and from the (HF-HL)-Ch computations are all in good agreement with laboratory data. The HF and HL models either yield reasonable distances, or fail grossly by not predicting any binding.² Comparing laboratory energies and the results of our HF-HL-Ch computations, we can set the error bar of this work at 0.5 kcal/mol.

In Tables 1 and 2 we present the $E_b(\text{model})$. In ref 2 we provided a table showing the similarities between MO orbitals and HL electron pairs; the two languages are below freely intermixed. We recall that the MO picture makes use for the X–H bond the $1\sigma_g^2$ for H₂, the $2\sigma^2$ for LiH, and for the remaining hydrides the $3\sigma^2$ orbital, more and more imbedded in the $2p_\pi$ electron cloud. For the HL model, the bond results from the formation of the electron pair $1s_{\text{Ha}}:1s_{\text{Hb}}$, $1s_{\text{H}}:2s_{\text{Li}}$, and $1s_{\text{H}}:2p\sigma_{\text{X}}$, respectively; both view points are utilized in the HF-HL model. The bonding orbital is formed with the 1s orbital from the H atom, a 2s orbital for the Li atom and a $2s-2p_\sigma$ hybrid for the hydrides BeH to HF.

Figure 1 displays the E_b pattern for the XH molecules, characterized by four maxima, specifically at H₂, LiH, BH, and HF, a plateau from BH to NH, and the two deep minima for HeH and NeH.

We start by considering HeH. The HF, HL, and HF-HL interactions are repulsive, and this is an indication that if there is a binding it will be notably weak. As we have noted in Section 3 for HeH, the ionic and excited configurations yield a minimum in the potential energy curve. We can be more specific and attempt to see how general is our understanding of the binding for hydrides. The $\text{He}^+ + \text{H}^-$ and the $\text{He}^- + \text{H}^+$ correlation energies are 0.03951 and 0.04204 hartree, to be compared to the HF-HL(1,1) molecular correlation of 0.04209 hartree at 6.65 bohr and 0.04207 at dissociation. Therefore, we expect a stabilization induced by the $\text{He}^- + \text{H}^+$ structure, with a distance shifted toward the Li united atom rather than toward dissociation. Indeed Figure 3 shows for the (HF-HL)_i curve a minimum at about 4.32 bohr. The addition of the $\text{He}(1s^1 2s^1)\text{H}(1s^1)$ covalent configuration accounts mainly for the atomic correlation, $\epsilon(\text{dyn})$ (the three orbitals 1s for H, 1s and 2s for He are different orbitals for different spins) as well as the excited covalent configuration with a 3s orbital on He. Thus, the van der Waals binding requires correlated atoms and to this it adds an ionic stabilization contribution.

The weak binding results from two competing and opposing effects: The covalent structures correlate mostly the dissociation

products, and marginally affect the energy at intermediate and short internuclear distances, thus a repulsive potential. The ionic structures bring about Coulombic (in general electrostatic, charge–charge, dipole–dipole, etc. interactions) stabilization at all distances vanishing toward dissociation. The sum of the two opposing contributions yields a weak minimum at large distances (atom to atom contact) where the electrostatic attraction prevails the covalent repulsion.

In our analysis the “atom to atom contact” is taken as the limiting (weakest) binding mechanism. We consider each XH bond as a specific situation within two limiting mechanism: at large distances the van der Waals limit and at zero distance the united atom limit (a clear Hartree–Fock model). The HF and the HL models are realized at intermediate distances, tending in the first situation to a united atom and the second, to van der Waals contacts.

The H₂ and the HF molecules appear to gain in $\eta_M(\text{dyn})$ stability by assuming an electronic structure compatible with the negative ion for HF and with $(\text{H}^+ + \text{H}^-)$ for H₂, both structures lead to the very stable atomic structures He and Ne at the united atom. The short equilibrium separation in H₂ and HF is therefore to be expected, like the notable improvement in the binding which results from adding the $\text{F}^- - \text{H}^+$ ionic structure to HF; the improvement from adding the $\text{H}^- - \text{H}^+$ structures to H₂ is modest (as expected), since the $\text{H}^- - \text{H}^+$ configuration does not imply an ionic character.

The H₂ laboratory value $E_b = 109.48$ kcal/mol is the first maximum of the bonding pattern in Figure 1 (with a “covalent homopolar bond”), lower only to the hydrogen fluoride value, the last maximum, with $E_b = 141.5$ kcal/mol (with an “ionic heteropolar bond”). These two bindings are the two highest in the XH molecules. For the HF molecule the HL compute binding energy is 92.17 kcal/mol near to the HL binding value of H₂, 94.28 kcal/mol. In the HF-HL approximation the two computed binding energy values differentiate: 94.50 kcal/mol for H₂ and 108.36 kcal/mol for HF; the Hartree–Fock component in the HF-HL model is more relevant in the HF molecule than in H₂, a trend already present in the computations with the Hartree–Fock model. However, it takes the introduction of “ionic structures” in the HL component to obtain a computed binding reasonably close to the laboratory data. Recall that in the H₂ molecule the ionic structure brings about simply “in–out” correlation, not charge transfer, and ionic binding as in HF.

From Figure 6 we learn that the LiH molecule would loose stability if it would assume a structure of the type $\text{Li}^- - \text{H}^+$ or be limited to Li–H, but gains with a structure of the type $\text{Li}^+ - \text{H}^-$. The structure $\text{Li}^+ - \text{H}^-$ is electronically equivalent to the van der Waals He₂ and the LiH large bond length can be taken as a consequence of this ionic contribution; the bond length, however, is shorter than expected for true van der Waals bonds because of the substantial binding energy from the HF, HL, and HF-HL models, 34.27, 43.11, and 43.66 kcal/mol, respectively. The inclusion of ionic structures brings the binding to 46.59 kcal/mol, a modest gain since the ionic structures are van der Waals type structures with weak bonding.

The binding in BeH is complicated by the molecule stability gained with the avoided state crossing² and by near-degeneracy in Be and Be⁻. The solution of the HF equation is a mixture of two solutions, one valid near equilibrium and a second near dissociation; this yields binding larger than the experimental value, 50.29 vs 49.84 kcal/mol; with “extensive rationalizations” we have tentatively suggested² for an Hartree–Fock binding of 40.20 kcal/mol. The HL model predicts a strong repulsion, but, finally the HF-HL model yields a binding of 40.50 kcal/

mol, a result in line with those from rest of the hydrides set. The binding energy is 45.73 kcal/mol after addition of the ionic structures.

From BH to HF the hydrides gain in stability by “being as similar as possible” to the corresponding atomic negative ion, as suggested by considering the molecular HF-HL binding (see Table 1), the improvements by addition of ionic structures (see Table 4), and the trends of the correlation energies (see Figure 6).

The three hydrides LiH, BH, and FH are in the $^1\Sigma^+$ state (the remaining hydrides differ either in the spin or in the angular momentum, and are considered below). Note that the binding energy of these three hydrides increases (see the Figure 1) essentially linearly, with the bond formed by the 1s orbital from the H atom and a $2s-2p_\sigma$ hybrid for F and B but a 2s orbital for the Li atom. The $(X^- + H^+)$ ionic structure is important for HF, less for BH; for LiH there is a switch to the $(X^+ + H^-)$ ionic structure. Recall from Figure 1 that the binding energy pattern is incorrectly given by the HF model and needs the HF-HL model to secure for LiH a binding larger than that of BeH; this trend is improved by considering the HF-HL model with ionic structures.

Finally we consider the binding energy plateau for CH, BH, and NH. Again Figure 1 provides an answer: the HF model predicts a net decrease from BH to CH to NH; the HF-HL model improves the overall binding but the incorrect slope remains. It takes consideration of the ionic structures to bring about a plateau.

Thus, from H–H to Ne–H we have illustrated an evolution in the binding character. The bond nomenclature, covalent for H₂, van der Waals for HeH, ionic from LiH to HF, and again van der Waals for NeH highlight the transitions within two extreme models, the united atom and the van der Waals contact. The obvious notion that atoms are the components of molecules brings about the corollary observation that the original atomic structure persists in the molecule subject to adaptations (the “perturbed atomic structure” of atoms in molecules), which allow optimal molecular stability sometime near dissociation, sometime at short internuclear distances, sometime at intermediate separations.

In the HF molecule, the F atom persists as F⁻ from near equilibrium to the united atom; in HeH and NeH the He and Ne atomic structures persist as a slightly perturbed atoms in contact with the hydrogen atom; in LiH the Li atom survives also as Li⁺ and the H atom as H⁻ yielding an incipient van der Waals situation; in the remaining hydrides the X atom survives as a negative ion.

Even if only preliminary, the above discussion demonstrates that the HF-HL model with DFA and the proto-models HF and HL and are sufficient to provide a reasonable physical and chemical understanding of the X–H bond. Further, it is evident that the HF and the HL models both are important but insufficient facets of the entire picture. Finally, we note that the discussion on the hydrides binding energy requires not only the HF, HL, and HF-HL models, and related correlation energies, but also consideration of the limiting conditions, namely the united and van der Waals contact.

The use of relatively short HF and HL expansions in the HF-HL model requires a qualification. Indeed, the advisability to reduce the size of canonical CI expansions and to use excitations to states physically more meaningful has led to the natural orbital concept, see for early examples refs 63–66. The HF-HL method, using not only the HF but also HL functions, is part of this trend.

7. Conclusion

For the atoms and molecules considered here, the HF energies are close to the exact nonrelativistic values; for the atoms, the HF energy is 99.5% of the exact total nonrelativistic energy, and for the molecules at equilibrium it is 99%. The HF binding energy is 63% of the experimental values (HeH and NeH not included). The HF-HL binding energies improve to 81%, and to 90% with inclusion of the ionic structures. The HF-HL-Ch brings total and binding energies to ~100%.

Thus, the observation that “the HF model needs a relatively small correction, E_c , to reach the exact nonrelativistic total energy”, has a complementary HF-HL observation: “the HF method is easily improved by adopting the HF-HL model, which dissociates correctly, accounts for near degeneracy, state crossing, and yields reasonable ab initio binding energies.” The remaining deviations from exact nonrelativistic energies are easily accounted with DFA. Note that in this paper we have selected the Coulomb hole functional,³⁴ but there are numerous alternative functionals. The HF-HL model present no problem in dealing correctly with excited states.⁹

In summary, the combination of the HF model^{3–7,10} with the HL model,⁸ namely, the HF-HL proposal,^{1,2} provides a simple ab initio physical model for a realistic representation of the electronic structure of molecular systems. These computations require only a few ab initio electronic configurations, and thus allow a simple, even if preliminary, rationalization on the nature of the chemical binding from van der Waals to very short internuclear distances.

Acknowledgment. It is my pleasure to thank Prof. Dr. Enrico Clementi for suggesting the topic, for discussions, for help in the manuscript preparation and for providing some of the computational facilities. I thank Prof. P. Bagus for discussion concerning the energy contamination at dissociation. The proofreading of the manuscript by Dr. Fiona Sim and a grant from MIUR-2004034838 are acknowledged.

References and Notes

- (1) Corongiu, G. *Int. J. Quantum Chem.* **2005**, *105*, 831.
- (2) Corongiu, G. *J. Phys. Chem A* **2006**, *110*, 11584.
- (3) Hartree, D. R. *Proc. R. Soc. London, Ser. A* **1933**, *141*, 269, and references thereby given.
- (4) Fock, V. *Z. Phys.* **1930**, *62*, 795.
- (5) Roothaan, C. C. J. *Rev. Mod. Phys.* **1951**, *23*, 69.
- (6) Roothaan, C. C. J. *Rev. Mod. Phys.* **1960**, *32*, 179.
- (7) Roothaan, C. C. J.; Bagus, P. S. *Methods Comput. Phys.* **1963**, *2*.
- (8) Heitler, W.; London, F. *Z. Phys.* **1927**, *44*, 455.
- (9) Corongiu, G. Manuscript to be submitted.
- (10) Hartree, D. R.; Hartree, W.; Swirles, B. *Trans. R. Soc.* **1939**, *299*, 238.
- (11) Sinanoglu, O. *J. Chem. Phys.* **1962**, *36*, 706.
- (12) Sinanoglu, O. *Adv. Chem. Phys.* **1964**, *6*, 305.
- (13) Veillard, A.; Clementi, E. *J. Chem. Phys.* **1969**, *44*, 3050.
- (14) Clementi, E. *J. Chem. Phys.* **1962**, *36*, 33.
- (15) Hiberty, P. C.; Humbel, S.; Byrman, C. P.; van Lenthe, J. H. *J. Chem. Phys.* **1994**, *101*, 5969.
- (16) Majorana, E. *Rend. Acc. Lincei* **1931**, *13*, 58.
- (17) Wigner, E.; Witmer, E. E. *Z. Physik* **1928**, *51*, 859.
- (18) Mulliken, R. S. *Rev. Mod. Phys.* **1932**, *4*, 1.
- (19) Herzberg, G. *Spectra of Diatomic Molecules*; D. Van Nostrand: Princeton, NJ, 1951, and references thereby given.
- (20) Huber, K. P.; Herzberg, G. *Molecular Spectra and Molecular Structure IV. Constants of Diatomic Molecules*; Van Nostrand Reinhold: New York, 1979.
- (21) Kołos, W.; Szalewicz, K.; Monkhorst, H. J. *J. Chem. Phys.* **1986**, *84*, 3278.
- (22) Gengenbach, R.; Hahn, C.; Toennies, J. P. *Phys. Rev. A* **1973**, *7*, 98.
- (23) Partridge, H.; Schwenke, D. W.; Bauschlicher, C. W. *J. Chem. Phys.* **1993**, *99*, 9776.
- (24) Colin, R.; Dreze, C.; Steinhauer, M. *Can. J. Phys.* **1983**, *61*, 641.

- (25) Persico, M. *Mol. Phys.* **1994**, *81*, 1463.
(26) Hofzumahus, A.; Stuhl, F. *J. Chem. Phys.* **1985**, *82*, 5519.
(27) Zemke, W. T.; Stwalley, W. C.; Coxon, J. A.; Hajigeorgiou, P. G. *Chem. Phys. Lett.* **1991**, *177*, 412.
(28) Chakravorty, S. J.; Davidson, E. R. *J. Phys. Chem.* **1996**, *100*, 616.
(29) Clementi, E.; Kraemer, W.; Salez, C. *J. Chem. Phys.* **1970**, *53*, 125.
(30) Clementi, E.; Corongiu, G. *Int. J. Quantum Chem.* **2005**, *105*, 709.
(31) Lie, G. C.; Clementi, E. *J. Chem. Phys.* **1974**, *60*, 1275.
(32) Lie, G. C.; Clementi, E. *J. Chem. Phys.* **1974**, *60*, 1288.
(33) Wang, S. G.; Schwarz, W. H. E. *J. Chem. Phys.* **1996**, *105*, 4641.
(34) Clementi, E. *IBM J. Res. Dev.* **1965**, *9*, 2.
(35) Clementi, E. *Proc. Natl. Acad. Sci. U.S.A.* **1972**, *69*, 2942, and reference thereby given.
(36) Wigner, E. *Phys. Rev.* **1934**, *46*, 1002.
(37) Gombas, P. *Die Statistische Theorie des Atoms und ihre Anwendungen*; Springer-Verlag: Wien, 1949.
(38) Gombas, P. *Pseudopotential*; Springer-Verlag: New York, 1967.
(39) Gombas, P. *Acta Phys.* **1961**, *13*, 233.
(40) Gombas, P. *Acta Phys.* **1962**, *14*, 83.
(41) Clementi, E.; Corongiu, G. In *Fundamental Aspects in Quantum Chemistry*; Kryachko, E. S., Brandas, E. J., Eds.; Kluwer Academic Publisher: Dordrecht, The Netherlands, 2003; p 601.
(42) Chakravorty, S.; Clementi, E. *Phys. Rev. A* **1989**, *39*, 2290.
(43) Clementi, E.; Corongiu, G. *Int. J. Quantum Chem.* **1997**, *62*, 572.
(44) Clementi, E.; Hofmann, D. W. *Int. J. Quantum Chem.* **1994**, *52*, 849.
(45) Clementi, E.; Corongiu, G. *Chem. Phys. Letters* **1998**, *282*, 335.
(46) Pisani, L.; Clementi, E. *J. Chem. Phys.* **1995**, *103*, 9321.
(47) Hohenberg, P.; Kohn, W. *Phys. Rev.* **1964**, *136B*, 864.
(48) See, for example: Parr, R. G.; Yang, W. *Density Functional Theory of Atoms and Molecules*; Oxford University Press: Oxford, 1985.
(49) Corongiu, G. To be published.
(50) Bagus, P. S. Private communication, February 2005.
(51) Colle, R.; Solvetti, O. *Theor. Chem. Acta (Berlin)* **1975**, *37*, 329.
(52) Gunnason, O.; Lundqvist, B.-I. *Phys. Rev. B* **1976**, *13*, 474.
(53) Vosko, S. H.; Wilk, L.; Nusair, M. *Can. J. Phys.* **1980**, *58*, 1200.
(54) Lagowsky, J. B.; Vosko, S. H. *J. Phys. B* **1988**, *21*, 203.
(55) Stoll, H.; Pavlidou, C. M. E.; Press, H. *Theor. Chim. Acta* **1978**, *49*, 143.
(56) Savin, A.; Stoll, H.; Preuss, H. *Theor. Chim. Acta* **1986**, *70*, 407.
(57) Perdew, J. P.; Zunger, A. *Phys. Rev. B* **1981**, *23*, 5048.
(58) Perdew, J. P. *Phys. Rev. B* **1986**, *33*, 8822.
(59) Becke, A. D. *J. Chem. Phys.* **1988**, *88*, 1053.
(60) Lee, C.; Yang, W.; Parr, R. G. *Phys. Rev. B* **1988**, *37*, 785.
(61) Clementi, E.; Chakravorty, S. *J. Chem. Phys.* **1990**, *93*, 2591.
(62) See for example Karplus, M.; Porter, R. N. *Atoms and Molecules. An Introduction for Students of Physical Chemistry*; W. A. Benjamin, Inc.: Menlo Park, CA, 1970.
(63) Löwdin, P.-O. *Phys. Rev.* **1955**, *97*, 1474.
(64) Bender, C. F.; Davidson, E. R. *J. Phys. Chem.* **1966**, *70*, 2675.
(65) Thulstrup, E. W.; Öhrn, Y. *J. Chem. Phys.* **1972**, *57*, 3716.
(66) Bagus, P. S.; Moser, C. M.; Goethals, P.; Verhagen, G. *J. Chem. Phys.* **1973**, *58*, 1886.